

# UC Irvine

## UC Irvine Previously Published Works

### Title

Search for  $n-n^{\bar{}}$  oscillation in Super-Kamiokande

### Permalink

<https://escholarship.org/uc/item/22f8s94g>

### Journal

Physical Review D, 91(7)

### ISSN

2470-0010

### Authors

Abe, K  
Hayato, Y  
Iida, T  
[et al.](#)

### Publication Date

2015-04-01

### DOI

10.1103/physrevd.91.072006

Peer reviewed

# Search for $n - \bar{n}$ oscillation in Super-Kamiokande

K. Abe,<sup>1</sup> Y. Hayato,<sup>1</sup> T. Iida,<sup>1</sup> K. Ishihara,<sup>1</sup> J. Kameda,<sup>1</sup> Y. Koshio,<sup>1</sup> A. Minamino,<sup>1</sup> C. Mitsuda,<sup>1</sup> M. Miura,<sup>1</sup> S. Moriyama,<sup>1</sup> M. Nakahata,<sup>1</sup> Y. Obayashi,<sup>1</sup> H. Ogawa,<sup>1</sup> H. Sekiya,<sup>1</sup> M. Shiozawa,<sup>1</sup> Y. Suzuki,<sup>1</sup> A. Takeda,<sup>1</sup> Y. Takeuchi,<sup>1</sup> K. Ueshima,<sup>1</sup> H. Watanabe,<sup>1</sup> I. Higuchi,<sup>2</sup> C. Ishihara,<sup>2</sup> M. Ishitsuka,<sup>2</sup> T. Kajita,<sup>2</sup> K. Kaneyuki,<sup>2,\*</sup> G. Mitsuka,<sup>2</sup> S. Nakayama,<sup>2</sup> H. Nishino,<sup>2</sup> K. Okumura,<sup>2</sup> C. Saji,<sup>2</sup> Y. Takenaga,<sup>2</sup> S. Clark,<sup>3</sup> S. Desai,<sup>3</sup> F. Dufour,<sup>3</sup> A. Herfurth,<sup>3</sup> E. Kearns,<sup>3</sup> S. Likhoded,<sup>3</sup> M. Litos,<sup>3</sup> J.L. Raaf,<sup>3</sup> J.L. Stone,<sup>3</sup> L.R. Sulak,<sup>3</sup> W. Wang,<sup>3,†</sup> M. Goldhaber,<sup>4,\*</sup> D. Casper,<sup>5</sup> J.P. Cravens,<sup>5</sup> J. Dunmore,<sup>5</sup> J. Griskevich,<sup>5</sup> W.R. Kropp,<sup>5</sup> D.W. Liu,<sup>5</sup> S. Mine,<sup>5</sup> C. Regis,<sup>5</sup> M.B. Smy,<sup>5</sup> H.W. Sobel,<sup>5</sup> M.R. Vagins,<sup>5</sup> K.S. Ganezer,<sup>6</sup> B. Hartfiel,<sup>6</sup> J. Hill,<sup>6</sup> W.E. Keig,<sup>6</sup> J.S. Jang,<sup>7</sup> I.S. Jeoung,<sup>7</sup> J.Y. Kim,<sup>7</sup> I.T. Lim,<sup>7</sup> K. Scholberg,<sup>8</sup> N. Tanimoto,<sup>8</sup> C.W. Walter,<sup>8</sup> R. Wendell,<sup>8</sup> R.W. Ellsworth,<sup>9</sup> S. Tasaka,<sup>10</sup> G. Guillian,<sup>11</sup> J.G. Learned,<sup>11</sup> S. Matsuno,<sup>11</sup> M.D. Messier,<sup>12</sup> A.K. Ichikawa,<sup>13</sup> T. Ishida,<sup>13</sup> T. Ishii,<sup>13</sup> T. Iwashita,<sup>13</sup> T. Kobayashi,<sup>13</sup> T. Nakadaira,<sup>13</sup> K. Nakamura,<sup>13</sup> K. Nishikawa,<sup>13</sup> K. Nitta,<sup>13</sup> Y. Oyama,<sup>13</sup> A.T. Suzuki,<sup>14</sup> M. Hasegawa,<sup>15</sup> H. Maesaka,<sup>15</sup> T. Nakaya,<sup>15</sup> T. Sasaki,<sup>15</sup> H. Sato,<sup>15</sup> H. Tanaka,<sup>15</sup> S. Yamamoto,<sup>15</sup> M. Yokoyama,<sup>15</sup> T.J. Haines,<sup>16</sup> S. Dazeley,<sup>17</sup> S. Hatakeyama,<sup>17</sup> R. Svoboda,<sup>17</sup> G.W. Sullivan,<sup>18</sup> R. Gran,<sup>19</sup> A. Habig,<sup>19</sup> Y. Fukuda,<sup>20</sup> Y. Itow,<sup>21</sup> T. Koike,<sup>21</sup> C.K. Jung,<sup>22</sup> T. Kato,<sup>22</sup> K. Kobayashi,<sup>22</sup> C. McGrew,<sup>22</sup> A. Sarrat,<sup>22</sup> R. Terri,<sup>22</sup> C. Yanagisawa,<sup>22</sup> N. Tamura,<sup>23</sup> M. Ikeda,<sup>24</sup> M. Sakuda,<sup>24</sup> Y. Kuno,<sup>25</sup> M. Yoshida,<sup>25</sup> S.B. Kim,<sup>26</sup> B.S. Yang,<sup>26</sup> T. Ishizuka,<sup>27</sup> H. Okazawa,<sup>28</sup> Y. Choi,<sup>29</sup> H.K. Seo,<sup>29</sup> Y. Gando,<sup>30</sup> T. Hasegawa,<sup>30</sup> K. Inoue,<sup>30</sup> H. Ishii,<sup>31</sup> K. Nishijima,<sup>31</sup> H. Ishino,<sup>32</sup> Y. Watanabe,<sup>32</sup> M. Koshihara,<sup>33</sup> Y. Totsuka,<sup>33,\*</sup> S. Chen,<sup>34</sup> Z. Deng,<sup>34</sup> Y. Liu,<sup>34</sup> D. Kielczewska,<sup>35</sup> H.G. Berns,<sup>36</sup> K.K. Shiraishi,<sup>36</sup> E. Thrane,<sup>36,‡</sup> K. Washburn,<sup>36</sup> and R.J. Wilkes<sup>36</sup>

(The Super-Kamiokande Collaboration)

<sup>1</sup>*Kamioka Observatory, Institute for Cosmic Ray Research, University of Tokyo, Kamioka, Gifu 506-1205, Japan*

<sup>2</sup>*Research Center for Cosmic Neutrinos, Institute for Cosmic Ray Research, University of Tokyo, Kashiwa, Chiba 277-8582, Japan*

<sup>3</sup>*Department of Physics, Boston University, Boston, MA 02215, USA*

<sup>4</sup>*Physics Department, Brookhaven National Laboratory, Upton, NY 11973, USA*

<sup>5</sup>*Department of Physics and Astronomy, University of California, Irvine, Irvine, CA 92697-4575, USA*

<sup>6</sup>*Department of Physics, California State University, Dominguez Hills, Carson, CA 90747, USA*

<sup>7</sup>*Department of Physics, Chonnam National University, Kwangju 500-757, Korea*

<sup>8</sup>*Department of Physics, Duke University, Durham NC 27708, USA*

<sup>9</sup>*Department of Physics, George Mason University, Fairfax, VA 22030, USA*

<sup>10</sup>*Department of Physics, Gifu University, Gifu, Gifu 501-1193, Japan*

<sup>11</sup>*Department of Physics and Astronomy, University of Hawaii, Honolulu, HI 96822, USA*

<sup>12</sup>*Department of Physics, Indiana University, Bloomington, IN 47405-7105, USA*

<sup>13</sup>*High Energy Accelerator Research Organization (KEK), Tsukuba, Ibaraki 305-0801, Japan*

<sup>14</sup>*Department of Physics, Kobe University, Kobe, Hyogo 657-8501, Japan*

<sup>15</sup>*Department of Physics, Kyoto University, Kyoto, Kyoto 606-8502, Japan*

<sup>16</sup>*Physics Division, P-23, Los Alamos National Laboratory, Los Alamos, NM 87544, USA*

<sup>17</sup>*Department of Physics and Astronomy, Louisiana State University, Baton Rouge, LA 70803, USA*

<sup>18</sup>*Department of Physics, University of Maryland, College Park, MD 20742, USA*

<sup>19</sup>*Department of Physics, University of Minnesota, Duluth, MN 55812-2496, USA*

<sup>20</sup>*Department of Physics, Miyagi University of Education, Sendai, Miyagi 980-0845, Japan*

<sup>21</sup>*Solar Terrestrial Environment Laboratory, Nagoya University, Nagoya, Aichi 464-8602, Japan*

<sup>22</sup>*Department of Physics and Astronomy, State University of New York, Stony Brook, NY 11794-3800, USA*

<sup>23</sup>*Department of Physics, Niigata University, Niigata, Niigata 950-2181, Japan*

<sup>24</sup>*Department of Physics, Okayama University, Okayama, Okayama 700-8530, Japan*

<sup>25</sup>*Department of Physics, Osaka University, Toyonaka, Osaka 560-0043, Japan*

<sup>26</sup>*Department of Physics, Seoul National University, Seoul 151-742, Korea*

<sup>27</sup>*Department of Systems Engineering, Shizuoka University, Hamamatsu, Shizuoka 432-8561, Japan*

<sup>28</sup>*Department of Informatics in Social Welfare, Shizuoka University of Welfare, Yaizu, Shizuoka, 425-8611, Japan*

<sup>29</sup>*Department of Physics, Sungkyunkwan University, Suwon 440-746, Korea*

<sup>30</sup>*Research Center for Neutrino Science, Tohoku University, Sendai, Miyagi 980-8578, Japan*

<sup>31</sup>*Department of Physics, Tokai University, Hiratsuka, Kanagawa 259-1292, Japan*

<sup>32</sup>*Department of Physics, Tokyo Institute for Technology, Meguro, Tokyo 152-8551, Japan*

<sup>33</sup>*The University of Tokyo, Bunkyo, Tokyo 113-0033, Japan*

<sup>34</sup>*Department of Engineering Physics, Tsinghua University, Beijing, 100084, China*

<sup>35</sup>*Institute of Experimental Physics, Warsaw University, 00-681 Warsaw, Poland*

<sup>36</sup>*Department of Physics, University of Washington, Seattle, WA 98195-1560, USA*

(Dated: April 16, 2015)

A search for neutron-antineutron ( $n - \bar{n}$ ) oscillation was undertaken in Super-Kamiokande using the 1489 live-day or  $2.45 \times 10^{34}$  neutron-year exposure data. This process violates both baryon and baryon minus lepton numbers by an absolute value of two units and is predicted by a large class of hypothetical models where the seesaw mechanism is incorporated to explain the observed tiny neutrino masses and the matter-antimatter asymmetry in the Universe. No evidence for  $n - \bar{n}$  oscillation was found, the lower limit of the lifetime for neutrons bound in  $^{16}\text{O}$ , in an analysis that included all of the significant sources of experimental uncertainties, was determined to be  $1.9 \times 10^{32}$  years at the 90% confidence level. The corresponding lower limit for the oscillation time of free neutrons was calculated to be  $2.7 \times 10^8$  s using a theoretical value of the nuclear suppression factor of  $0.517 \times 10^{23} \text{ s}^{-1}$  and its uncertainty.

PACS numbers: 11.30.Fs, 12.10.Dm, 14.20.Dh, 29.40.Ka

## I. INTRODUCTION

Searches for baryon number ( $B$ ) violating processes are motivated by various grand unification theories (GUTs) and by the observation first put forward by A. Sakharov in 1967 that  $B$ ,  $C$ ,  $CP$  violation, and nonequilibrium thermodynamics are needed to explain the observed matter-antimatter or baryon number asymmetry of the Universe [1]. However recent experimental limits on  $p \rightarrow e^+ \pi^0$  [2–4] and  $p \rightarrow \bar{\nu} K^+$  [5] have already ruled out the simplest  $B-L$  conserving GUTs, minimal  $SU(5)$  and the minimal supersymmetric version of  $SU(5)$ , where  $L$  stands for lepton number. It has also been shown that any  $B-L$  conserving baryon asymmetry generated in the early Universe (above 10 TeV scale) should be washed out until now by the triangle anomalies involving electroweak bosons. Therefore the search for  $B-L$  violating reactions has become increasingly important as a potential explanation of the observed baryon number asymmetry in the Universe.

Neutron-antineutron ( $n - \bar{n}$ ) oscillation, a process that violates  $B$  and  $B-L$  by two units ( $|\Delta B| = 2$  and  $|\Delta(B-L)| = 2$ ), was first discussed by V. Kuzmin in 1970 [6]. The discovery of neutrino oscillations [7] has renewed interest in theories with Majorana spinors which yield  $B$  and  $L$  symmetry breaking by allowing  $|\Delta(B-L)| = 2$ , with  $|\Delta L|=2$  as in neutrinoless double beta decay and  $|\Delta B|=2$  for  $n - \bar{n}$  oscillation [8, 9]. These models include a large class of supersymmetric and right-left symmetric  $SU(2)_L \otimes SU(2)_R \otimes SU(4)_C$  theories that include the seesaw mechanism to generate neutrino masses [10]. Neutron-antineutron oscillation has also been predicted by GUTs with large or small extra space-time dimensions [11, 12].

An important property of  $n - \bar{n}$  oscillation is its dependence on a six quark operator, with a mass scaling of  $M^{-5}$  instead of  $M^{-2}$  as in the charged  $X$  and  $Y$  bosons that mediate nucleon decay in minimal  $SU(5)$ . There-

fore, the observation of a significant  $n - \bar{n}$  oscillation signal at Super-Kamiokande would imply new physics at a scale of approximately 100 TeV, a factor of 10 larger than the maximum energies scheduled for study at the Large Hadron Collider.

The previous best 90 % confidence level (C.L.) lifetime limits for bound neutrons are from IMB with 1.7 and  $2.4 \times 10^{31}$  year [13] in two different analyses, Kamiokande with  $4.3 \times 10^{31}$  year in oxygen [14], Soudan 2 with  $7.2 \times 10^{31}$  year in iron [15], and Frejus with  $6.5 \times 10^{31}$  year in iron [16]. The current best limit on the oscillation time of unbound neutrons is given by ILL (Grenoble) as  $0.86 \times 10^8$  seconds [17]. The lifetime limit for bound neutrons can be converted to the  $n - \bar{n}$  oscillation time for free neutrons by the relationship

$$T_{n-\bar{n}} = R \cdot \tau_{n-\bar{n}}^2 \quad (1)$$

where  $\tau_{n-\bar{n}}$  and  $T_{n-\bar{n}}$  are the oscillation time of a free neutron and the lifetime of a bound neutron, and  $R$  is the nuclear suppression factor, for which theoretical estimates are given in the literature [18].

In this paper, we describe the results of our neutron-antineutron oscillation search in Super-Kamiokande. No positive signal was observed, but from our data we obtained a lower limit on the lifetime of a neutron in oxygen of  $1.9 \times 10^{32}$  year (90% C.L.), which is about four times larger than the previous highest experimental limits.

## II. THE SUPER-KAMIOKANDE DETECTOR

Super-Kamiokande is a ring imaging water Cherenkov detector containing 50 ktons of ultrapure water, located in Kamioka-town in Gifu prefecture, Japan. The detector is composed of the inner detector, which contains 22.5 kton fiducial volume, and the outer detector for tagging cosmic ray muons entering the detector. Descriptive overviews of Super-Kamiokande and technical details are given in the literature [19]. The  $n - \bar{n}$  oscillation analysis described in this paper uses the complete Super-Kamiokande-I data set, which is equivalent to  $2.45 \times 10^{34}$  neutron-year exposure data. This data set of 1489 live-days was taken from May 31, 1996 to July 15, 2001.

An antineutron is expected to annihilate quickly with one of the surrounding nucleons and to produce multiple

\* Deceased.

† Present address: Department of Physics, University of Wisconsin-Madison, 1150 University Avenue Madison, WI 53706

‡ Present address: Department of Physics and Astronomy, University of Minnesota, MN, 55455, USA

secondary hadrons, mainly pions. The total momentum of the secondaries is nearly zero, except for the Fermi momenta of the annihilating  $\bar{n}$  and nucleon, and the total energy is nearly equal to the total mass of the two nucleons. Therefore in the case of no nuclear interactions it was expected that  $n - \bar{n}$  oscillation events in oxygen would produce mesons with a total energy of about 2 GeV, distributed isotropically.

### III. MONTE CARLO SIMULATION

A detailed Monte Carlo (MC) simulation was formulated for this study. Since the literature on ( $\bar{n} + \text{nucleon}$ ) annihilation in nuclei is sparse,  $\bar{p}p$  and  $\bar{p}d$  data from hydrogen and deuterium bubble chambers [20–22] were used to determine the branching ratios for the annihilation final states. The branching ratios included in our simulations are displayed in Table I. The values of kinematic quantities in our MC were determined using relativistic phase-space distributions that included the Fermi momentum of the annihilating nucleons. Pions and omegas produced in the  $\bar{n}$ -nucleon annihilations were propagated through the residual nucleus. This study used a program originally developed for the IMB experiment to simulate meson-nucleon interactions [13]. The cross sections for the pion-residual nucleus interactions were based on an interpolation from measured pion-carbon and pion-aluminum cross sections to those for pion- $^{16}\text{O}$  interactions. Excitation of the  $\Delta(1232)$  resonance was the most important effect in the nuclear propagation phase. It was assumed that the pion and omega cross sections scaled linearly with matter density, a quantity that decreases as the mesons move away from the annihilation point and exit from the nucleus. The Fermi momentum of the interacting nucleon and the possibility of Pauli blocking were also included in our simulations. We found that 49% of the pions did not interact, while 24% were absorbed and 3% interacted with a nucleon to produce an additional pion or occasionally two more pions, and the rest of the pion interactions involved scattering. These interaction probabilities yielded total and charged pion multiplicities of 3.5 and 2.2, respectively, with an average charged pion momentum of 310 MeV/ $c$  and a root mean square width of 190 MeV/ $c$ . There was a probability of 0.56% that an event included an  $\omega^0$  that emerged from the nucleus without having decayed. The final states of the nuclear fragments were calculated using an algorithm based on a simulation from Oak Ridge National Laboratory [23]. Fragments of the residual nucleus that contained two or more nucleons were not simulated in water, since most of the nucleons in these fragments had momenta that were below the threshold for inelastic hadron interactions. Therefore only free  $n$  and  $p$  fragments were propagated through water.

Since the largest source of background events for  $n - \bar{n}$  oscillation is atmospheric neutrinos, we prepared a large MC event sample that corresponded to an atmospheric

neutrino exposure of 500 years. A detailed description of this simulation is given in reference [24]. The propagation of particles and Cherenkov light in the detector was modeled by a program that is based on the GEANT-3 package [25]. The detector geometry, the generation and propagation of Cherenkov radiation from charged particles, and the response of the photomultiplier tubes (PMTs) and data acquisition electronics were also included in our simulations. Hadron interactions were simulated using the CALOR package [26] for nucleons and charged pions with  $p_\pi > 500$  MeV/ $c$ , and through a custom-made program [27] for charged pions of  $p_\pi < 500$  MeV/ $c$ .

TABLE I. The branching ratios for the  $\bar{n}$ +nucleon annihilations in our simulations. These factors were derived from  $\bar{p}p$  and  $\bar{p}d$  bubble chamber data[20–22].

$\bar{n}+p$		$\bar{n}+n$	
$\pi^+\pi^0$	1%	$\pi^+\pi^-$	2%
$\pi^+2\pi^0$	8%	$2\pi^0$	1.5%
$\pi^+3\pi^0$	10%	$\pi^+\pi^-\pi^0$	6.5%
$2\pi^+\pi^-\pi^0$	22%	$\pi^+\pi^-2\pi^0$	11%
$2\pi^+\pi^-2\pi^0$	36%	$\pi^+\pi^-3\pi^0$	28%
$2\pi^+\pi^-2\omega$	16%	$2\pi^+2\pi^-$	7%
$3\pi^+2\pi^-\pi^0$	7%	$2\pi^+2\pi^-\pi^0$	24%
		$\pi^+\pi^-\omega$	10%
		$2\pi^+2\pi^-2\pi^0$	10%

### IV. DATA REDUCTION AND RECONSTRUCTION

The trigger threshold for our search corresponds to 5.7 MeV of electromagnetic energy, therefore signal events would trigger with 100% efficiency. The majority of triggered events in the Super-Kamiokande data are background due to inherent radioactivity or to cosmic ray muons passing in the detector. Most of the cosmic ray muon events are rejected by a requirement that the number of hit PMTs in the outer detector within 800 ns of the trigger be less than 25. We also require that the reconstructed visible energy be greater than 30 MeV to remove the remaining low energy radioactivity. This constraint is also necessary to maintain the effectiveness of the event reconstruction. The reduction algorithms are identical to those used for the atmospheric neutrino analyses and nucleon decay searches [24].

Events remaining after the reduction procedure are processed by the full reconstruction program, which yields an overall event vertex, the number of Cherenkov rings, and a direction, particle identification determination, and a momentum for each ring [24]. For  $n - \bar{n}$  oscillation events the vertex resolution is 26 cm. Each

Cherenkov ring is identified as being either “showering” ( $e, \gamma$ ) or “nonshowering” ( $\mu, \pi, p$ ) based upon its hit pattern and opening angle. The momentum is subsequently determined using the assigned particle type and the number of collected photoelectrons inside a cone with an opening half-angle of 70 degrees after corrections for geometric effects and light attenuation are made. Our choice of cone angle completely covers the Cherenkov cone in water, which has an opening half-angle of about 42 degrees. In multiple-Cherenkov ring events, we estimate and separate a sample of photoelectrons for each ring using an expected Cherenkov light distribution.

## V. ANALYSIS

To isolate  $n - \bar{n}$  candidates we apply additional criteria to the fully contained (FC) event sample within the inner detector; this sample is used for our atmospheric neutrino analyses and nucleon decay searches [24]. In addition, we require the following:

(a) The number of Cherenkov rings  $> 1$ , (b)  $700 \text{ MeV} < \text{Visible energy} < 1300 \text{ MeV}$ , (c)  $0 \text{ MeV}/c < \text{Total momentum} < 450 \text{ MeV}/c$  and (d)  $750 \text{ MeV}/c^2 < \text{Invariant mass} < 1800 \text{ MeV}/c^2$ . The visible energy is defined as the energy of an electron that would produce the same total amount of light in the detector. The total momentum is  $P_{\text{tot}} = |\sum_i^{\text{all-rings}} \vec{p}_i|$ , where  $\vec{p}_i$  is the reconstructed momentum vector of the  $i$ th ring. The invariant mass is defined to be  $M_{\text{tot}} = \sqrt{E_{\text{tot}}^2 - P_{\text{tot}}^2}$ , while the total energy is defined as  $E_{\text{tot}} = \sum_i^{\text{all-rings}} \sqrt{p_i^2 + m_i^2}$ , where  $m_i$  is the mass of the  $i$ th ring assuming that showering and nonshowering rings are from  $\gamma$  rays and charged pions, respectively. The selection criteria given above were optimized to maximize the ratio  $\epsilon/\sqrt{b}$ , where  $\epsilon$  is the signal detection efficiency and  $b$  is the number of background events.

Distributions of the four reconstructed kinematic variables are displayed in Fig. 1. Our atmospheric neutrino MC includes the effects of  $\nu_\mu$  to  $\nu_\tau$  neutrino oscillations, with mixing parameters of  $(\sin^2 2\theta, \Delta m^2) = (1.0, 2.1 \times 10^{-3} \text{ eV}^2)$  obtained from our publication on this topic [24]. Figure 1 (b) shows the visible energy distribution after the event selection criterion (a) based on the number of Cherenkov rings was imposed. The average visible energy for  $n - \bar{n}$  MC oscillation events is about 700 MeV, much lower than twice the nucleon mass. The reasons for observing lower visible energy include the mass of charged mesons, energy loss by mesons scattering off nucleons, and the absorption of mesons in nuclear reactions. The visible energy would approach twice the nucleon mass only if the annihilation resulted fully in electromagnetic showers (such as multiple  $\pi^0$  that decayed before interaction).

Application of the event selection criteria (a)-(d) yielded 24 candidate events, a detection efficiency of 12.1% from the remaining  $n - \bar{n}$  MC events in the final sample, and 24.1 background events as estimated for

the 1489 days of Super-Kamiokande-I. Final event samples are displayed as scattered dots inside of the box-shaped scatterplots that apply criteria (c)-(d) in Fig. 2. Of the remaining background, 57.8% comes from multihadron production by deep inelastic scattering (DIS), 31.4% from single pion production via resonances, and 5.5% from single  $\eta$  and  $K$  meson production via resonances. The remaining 5.2% of the background results from charged current (CC) quasielastic (QE) scattering and neutral current (NC) elastic scattering accompanied by energetic knocked-out nucleons in the water.

## VI. SYSTEMATIC ERRORS

Uncertainties in the detection efficiency, exposure, and background rates are given in Table II. The major sources of errors in the detection efficiency are the results of uncertainties in the models for propagation of pions and omega mesons through the residual nucleus. In particular, the error due to uncertainties in the  $\pi$ -nucleon cross section is 20.0%, as estimated from the  $\pi$ - $^{16}\text{O}$  scattering data shown in [13] and by comparing results from two independent nuclear interaction programs originally developed by IMB [13] and by Kamiokande [14] (6.1%). The uncertainty from the  $(\bar{n} + \text{nucleon})$  annihilation branching ratios is estimated to be 4.6% by comparing different MC results based on variations in the assumed branching ratios [28, 29]. The 0.6% asymmetry in the detector gain and the 2.0% difference in the energy scale between the data and the MC would affect the momentum cut and contribute 1.7% and 0.4% uncertainties, respectively. By comparing real data with MC events we estimate that the uncertainty in the Cherenkov ring finding procedure is 2.2%. The detection efficiency is estimated to have a total uncertainty of 22.9% while the exposure uncertainty was found to be 3.0% through an estimate of the error in the calculation of the effective fiducial volume.

The uncertainties in the atmospheric neutrino flux, the atmospheric neutrino energy spectrum, and the components of the atmospheric neutrino flux contribute 7.8% to the systematic uncertainty of the background rate. The DIS cross section uncertainty in the low  $q^2$  region yields a large contribution to the uncertainty in the background rate, which is estimated to be 14.1% by comparing the results from two different parametrizations of the parton distribution functions [30, 31]. The uncertainty in the energy scale, the lack of perfect uniformity in the PMT gain, and the uncertainty in the Cherenkov ring finding contribute a total of 14.9% to the systematic errors. The total systematic uncertainty in the background rate is estimated to be 23.7%.

## VII. RESULTS

No significant excess was found in our full 1489 day Super-Kamiokande-I data set. The lower limit on the life-

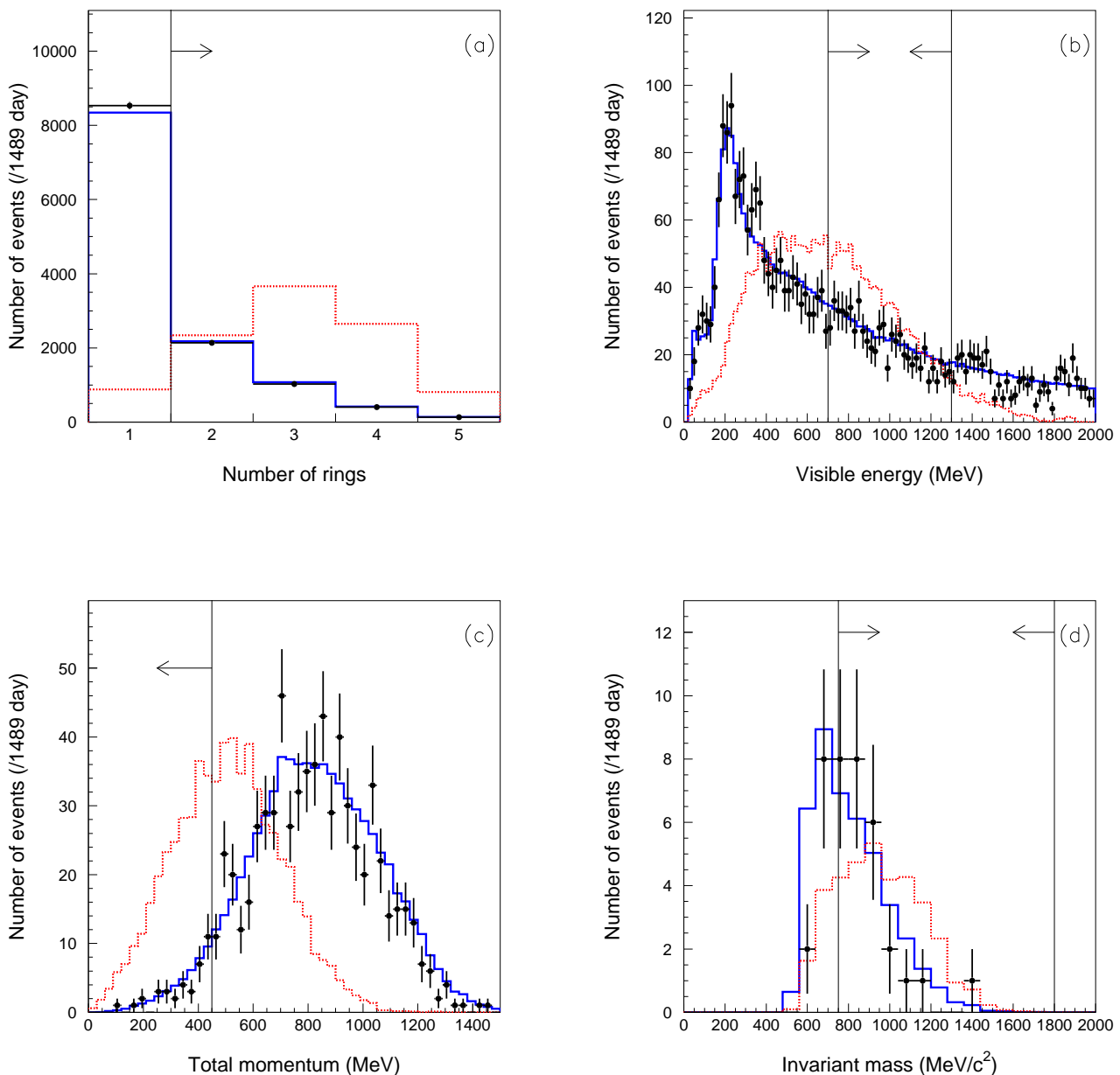


FIG. 1. (color online) The distributions of the kinematic variables subject to additional criteria at each of the reduction steps described in the text including: (a) number of rings, (b) visible energy, (c) total momentum, and (d) invariant mass. Circles indicate data points with statistical error bars; solid blue lines and dashed red lines represent the atmospheric neutrino MC and the  $n - \bar{n}$  MC, respectively. Light vertical lines with arrows indicate the event selection criteria.

time of a neutron bound inside an oxygen nucleus due to  $n - \bar{n}$  oscillation was calculated from the 24 observed candidate and 24.1 expected background events. All of the systematic uncertainties were included in the limit calculation by employing the Bayesian statistical method [32]

as follows:

$$P(\Gamma|n_{\text{obs}}) = A \int \int \int \frac{e^{-(\Gamma\lambda\epsilon+b)} (\Gamma\lambda\epsilon+b)^{n_{\text{obs}}}}{n_{\text{obs}}!} \times P(\Gamma)P(\lambda)P(\epsilon)P(b)d\lambda d\epsilon db. \quad (2)$$

The above normalization constant  $A$  in Eq. (2) was determined by imposing the constraint  $\int_0^\infty P(\Gamma|n_{\text{obs}})d\Gamma = 1$

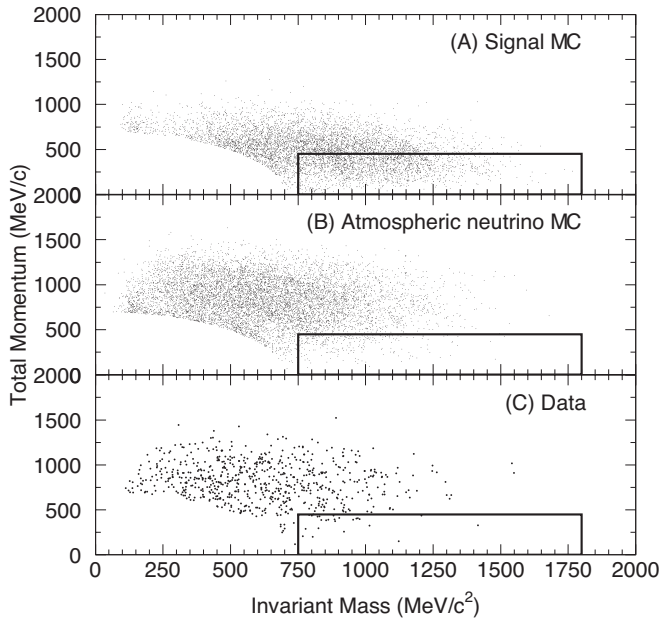


FIG. 2. Total momentum vs the invariant mass after applying the selection criteria (a)-(b) on the FC sample: (A) signal MC, (B) atmospheric neutrino MC, and (C) data. The boxed region in each panel shows the criterion (c)-(d) for the  $n - \bar{n}$  oscillation signal.

where  $\Gamma$ ,  $\lambda = NT$ , and  $\epsilon$  are the true values of the event rate, exposure, and detection efficiency, respectively, for  $n - \bar{n}$  oscillation.  $N$  and  $T$  are the number of neutrons and the live-days,  $n_{\text{obs}} = 24$  is the number of observed candidates, and  $b$  is the true mean number of background events.  $P(\Gamma), P(\lambda), P(\epsilon), P(b)$  in Eq. (2) are the prior probability density functions, which we assume are Gaussian distributions for  $\lambda$ ,  $\epsilon$ , and  $b$ .  $P(\Gamma)$  is a flat distribution for  $\Gamma \geq 0$  and 0 for negative  $\Gamma$ . Finally, the 90% C.L. limit of the neutron lifetime for  $n - \bar{n}$  oscillation in oxygen with the inclusion of systematic uncertainties is determined from Eqs. (3)-(4) as follows:

$$T_{n-\bar{n}} = 1/\Gamma_{\text{limit}}, \quad (3)$$

$$\text{C.L.} = \int_0^{\Gamma_{\text{limit}}} P(\Gamma|n) d\Gamma \quad (4)$$

where C.L.=0.9. The calculated result is

$$T_{n-\bar{n}} > 1.9 \times 10^{32} \text{ years.} \quad (5)$$

This lifetime for oscillation of a bound neutron is converted to the  $n - \bar{n}$  oscillation time of a free neutron using Eq. (1). The result depends on the choice of the nuclear suppression factor,  $R$ . A straightforward application of Eq. (1), using our result in Eq. (5) and the older suppression factor  $R = 1.0 \times 10^{23} \text{ s}^{-1}$  yields a limit on the free neutron oscillation time of  $> 2.4 \times 10^8$  seconds. This may be directly compared with the deduced free neutron limits from Kamiokande and IMB, as listed

TABLE II. Systematic uncertainties in the signal efficiency, exposure, and background rate.

Signal efficiency	
Sources	Uncertainty (%)
Fermi momentum of nucleons	6.2
Branching ratio of $\bar{n}$ +nucleons	4.6
$\pi$ propagation modeling	6.1
$\pi$ -nucleon cross section in the nucleus	20.0
Energy scale	1.7
Asymmetry of detector gain	0.4
Cherenkov ring finding	2.2
Total	22.9
Exposure	
Sources	Uncertainty (%)
Fiducial volume	3.0
Detector live-days	<0.1
Total	3.0
Background rate	
Sources	Uncertainty(%)
$(\nu_e + \bar{\nu}_e)/(\nu_\mu + \bar{\nu}_\mu)$ , $\nu/\bar{\nu}$ ratio	0.1, 1.0
Up/down, horizontal/vertical flux ratios	$\ll 1$
$K/\pi$ ratio	3.1
Neutrino energy spectrum (<1, >1GeV)	6.1,3.6
Neutrino cross sections	
QE	5.8
1- $\pi$ production	2.4
DIS	14.1
coherent $\pi$ productions	$\ll 1$
CC/NC cross section ratio	5.0
Axial vector mass in QE and 1 $\pi$ prod.	0.6
Fermi momentum for QE	$\ll 1$
$\pi$ propagation in $^{16}\text{O}$	4.1
Energy scale	4.8
Asymmetry of detector gain	0.5
Cherenkov ring finding	14.1
Total	23.7

in Table III, which used the same nuclear suppression factor. Since the time of those experiments, Friedman and Gal have published an improved calculation of the nuclear suppression factor [18]. Their calculation uses nuclear potentials based on recent data [33], resulting in a significantly lower value of:

$$R = 0.517 \times 10^{23} \text{ s}^{-1}, \quad (6)$$

with a theoretical uncertainty of 20–30% [18]. We note that the earlier value of  $R$  is well outside this theoretic-

TABLE III. A comparison of the Super-Kamiokande results with those of previous  $n - \bar{n}$  experiments using bound neutrons [13–16]. The abbreviation SK, SD2, and KAM stands for Super-Kamiokande, Soudan 2, and Kamiokande, respectively.

Experiment	SK	SD2	Frejus	KAM	IMB
Source of neutrons	Oxygen	Iron	Iron	Oxygen	Oxygen
Exposure ( $10^{32}$ neutron-yr)	245	21.9	5.0	3.0	3.2
Efficiency(%)	12.1	18.0	30.0	33.0	50.0
Candidates	24	5	0	0	3
Backgrounds	24.1	4.5	2.5(2.1)	0.9	–
$T_{n-\bar{n}}$ ( $10^{32}$ yr)	1.9	0.72	0.65	0.43	0.24
Suppression factor ( $10^{23}$ sec $^{-1}$ )	0.517	1.4	1.4	1.0	1.0
$\tau_{n-\bar{n}}$ ( $10^8$ sec)	2.7	1.3	1.2	1.2	0.88

cal uncertainty, but simply take the latest estimate and its uncertainty at face value for interpreting our result. The application of Eqs. (1) and (5) with this value of  $R$  results in a limit on the free neutron oscillation time of  $\tau_{n-\bar{n}} > 3.4 \times 10^8$  s at the 90% C.L. We take account of the theoretical uncertainty of 30% in  $R$  by applying the same Bayesian treatment using Eq. (2) to the normalization. With this consideration, the free neutron lifetime is more conservatively limited to be:

$$\tau_{n-\bar{n}} > 2.7 \times 10^8 \text{ s} \quad (7)$$

at the 90% C.L. This limit represents the best understanding that may be derived from our search and can be compared to the direct result on free neutron oscillation from the ILL/Grenoble experiment [17],  $\tau_{n-\bar{n}} > 0.86 \times 10^8$  seconds.

## VIII. SUMMARY

We have searched for neutron-antineutron oscillation with  $2.45 \times 10^{34}$  neutron-years of exposure of  $^{16}\text{O}$  in the Super-Kamiokande-I experiment. A small number of simple selection criteria were employed and the search window in total momentum versus invariant mass was optimized for this exposure. Twenty-four events pass the selection criteria, but the estimated background was  $24.1 \pm 5.7$  events, and the distribution of events agrees with the expectation from atmospheric neutrino interactions. The signal efficiency was  $12.1 \pm 2.8\%$ . We performed a limit calculation that incorporates systematic uncertainties, arriving at a bound lifetime limit of  $T_{n-\bar{n}} > 1.9 \times 10^{32}$  years. This is more than four times greater than the best limit from a water Cherenkov experiment, despite having nearly eighty times the exposure because these searches are background limited. Using a recent calculation of the nuclear suppression factor, the negative results of our search for  $n - \bar{n}$  oscillation in  $^{16}\text{O}$  is equivalent to a limit for free  $n - \bar{n}$  oscillation time of greater than  $2.7 \times 10^8$  seconds. This result is three times more restrictive than the ILL/Grenoble reactor experiment. This places strict limitations on ( $\Delta B = 2$ ,  $\Delta L = 0$ ) processes in physics beyond the standard model.

## ACKNOWLEDGMENTS

We gratefully acknowledge the cooperation of the Kamioka Mining and Smelting Company. The Super-Kamiokande experiment was built from, and has been operated with, funding by the Japanese Ministry of Education, Science, Sports and Culture, and the United States Department of Energy. We also would like to express our gratitude to the following agencies for their support of our research; the U.S. National Science Foundation (including Grants No. PHY 0401139 and No. PHY 0901048 to CSUDH), the National Research Foundation of Korea (Grant No. NRF-2009-353-C00046), and the National Natural Science Foundation of China.

- 
- [1] A. D. Sakharov, Violation of  $CP$  Invariance,  $C$  Asymmetry, and Baryon Asymmetry of the Universe, Pis'ma Zh. E'ksp. Teor. Fiz. **5**, 32 (1967) [JETP Lett. **5**, 24 (1967)].
  - [2] C. McGrew *et al.* (IMB-3 Collaboration), Search for nucleon decay using the IMB-3 detector, Phys. Rev. D **59**, 052004 (1999).
  - [3] K. Hirata *et al.* (Kamiokande-II Collaboration), Experimental limits on nucleon lifetime for lepton+meson decay modes, Phys. Lett. B **220**, 308 (1989).
  - [4] M. Shiozawa *et al.* (Super-Kamiokande Collaboration), Search for Proton Decay via  $p \rightarrow e^+\pi^0$  in a Large Water Cherenkov Detector, Phys. Rev. Lett. **81**, 3319 (1998); H. Nishino *et al.* (Super-Kamiokande Collaboration), Search for Nucleon Decay into Charged Anti-lepton plus Meson in Super-Kamiokande I and II, Phys. Rev. D **85**, 112001 (2012).
  - [5] K. Kobayashi *et al.* (Super-Kamiokande Collaboration), Search for nucleon decay via modes favored by supersymmetric grand unification models in Super-Kamiokande-I, Phys. Rev. D **72**, 052007 (2005).
  - [6] V. A. Kuzmin,  $CP$  violation and baryon asymmetry of the universe, Pis'ma Zh. E'ksp. Teor. Fiz. **12**, 335 (1970) [JETP Lett. **12**, 228 (1970)].
  - [7] Y. Fukuda *et al.* (Super-Kamiokande Collaboration), Evidence for oscillation of atmospheric neutrinos, Phys. Rev. Lett. **81**, 1562 (1998).
  - [8] R. N. Mohapatra, Neutron-anti-neutron oscillation: theory and phenomenology, J. Phys G **36**, 104006 (2009).



- [9] D. G. Phillips, II, W. M. Snow, K. Babu, S. Banerjee, D. V. Baxter, Z. Berezhiani, M. Bergevin and S. Bhattacharya *et al.*, Neutron-Antineutron Oscillations: Theoretical Status and Experimental Prospects, arXiv:1410.1100 [Phys. Rep. (to be published)].
- [10] K. S. Babu and R. N. Mohapatra, Observable neutron-antineutron oscillations in seesaw models of neutrino mass, Phys. Lett. B **518**, 269 (2001).
- [11] S. Nussinov and R. Shrock,  $n - \bar{n}$  Oscillations in Models with Large Extra Dimensions, Phys. Rev. Lett. **88**, 171601 (2002).
- [12] S. J. Huber and Q. Shafi, Neutrino oscillations and rare processes in models with a small extra dimension, Phys. Lett. B **512**, 365 (2001).
- [13] T. W. Jones *et al.* (IMB Collaboration), Search for  $n - \bar{n}$  Oscillation in Oxygen, Phys. Rev. Lett. **52**, 720 (1984).
- [14] M. Takita *et al.* (Kamiokande Collaboration), Search for neutron-antineutron oscillation in  $^{16}\text{O}$  nuclei, Phys. Rev. D **34**, 902-904 (1986).
- [15] J. Chung *et al.* (Soudan 2 Collaboration), Search for neutron-antineutron oscillations using multiprong events in Soudan 2, Phys Rev D **66**, 032004 (2002).
- [16] C. Berger *et al.* (Frejus Collaboration), Search for Neutron - Antineutron Oscillations in the Frejus Detector, Phys. Lett. B **240**, 237 (1990).
- [17] M. Baldo-Ceolin *et al.*, A new experimental limit on neutron-antineutron oscillations, Z. Phys. C **63**, 409-416 (1994).
- [18] E. Friedman and A. Gal, Realistic calculations of nuclear disappearance lifetimes induced by  $n\bar{n}$  oscillations, Phys. Rev. D **78**, 016002 (2008).
- [19] Y. Fukuda *et al.*, (Super-Kamiokande Collaboration), The Super-Kamiokande detector, Nucl. Instrum. Meth. A **501**, 418-462 (2003).
- [20] R. Armenteros and B. French, Antinucleon-Nucleon Interactions, *High Energy Physics* (Academic, New York, 1969), Vol.4, p.237.
- [21] P. Pavlopoulos *et al.*, Possible evidence for narrow bound states related to the  $p\bar{p}$  system, AIP Conf. Proc. **41**, 340 (1978).
- [22] A. Backenstoss *et al.*, Proton - Anti-proton Annihilations at Rest Into  $\pi^0\omega$ ,  $\pi^0\eta$ ,  $\pi^0\gamma$ ,  $\pi^0\pi^0$ , and  $\pi^0\eta'$ , Nucl. Phys. B **228**, 424 (1983).
- [23] Ye. S. Golubeva, A. S. Iljinov, and L. A. Kondratyuk, Antineutron Annihilation Event Generator for  $n - \bar{n}$  Search Experiment, ORNL-6910, in *Proceedings of the International Workshop on Future Prospects of Baryon Instability Search in  $p$ -Decay and  $n - \bar{n}$  Oscillation Experiments, Oak Ridge Tennessee, 1996*, p. 295.
- [24] Y. Ashie *et al.*, (Super-Kamiokande Collaboration), Measurement of atmospheric neutrino oscillation parameters by Super-Kamiokande I, Phys. Rev. D, **71**, 112005 (2005).
- [25] R. Brun and F. Carminati, GEANT Detector Description and Simulation Tool, CERN Program Library Long Wwriteup W5013 (1993).
- [26] T. A. Gabriel, J. E. Brau, and B. L. Bishop, The physics of compensating calorimetry and the new Calor89 code system, IEEE Trans. Nucl. Sci. **36**, 14 (1989).
- [27] M. Nakahata *et al.*, (Kamiokande Collaboration), Atmospheric Neutrino Background and Pion Nuclear Effect for KAMIOKA Nucleon Decay Experiment, J. Phys. Soc. Jpn. **55**, 3786 (1986).
- [28] C. Baltay, P. Franzini, G. Lütjen, J. C. Severiens, D. Tycko and D. Zanello, Annihilations of Antiprotons at Rest in Hydrogen. V. Multipion Annihilations, Phys. Rev. **145**, 1103 (1966).
- [29] A. Bettini *et al.*, Annihilation into pions of the  $\bar{p}n$  system from antiprotons at rest in deuterium, Nuovo Cimento **47**, 642 (1967).
- [30] M. Glück, E. Reya, and A. Vogt, Dynamical parton distributions revisited, Eur. Phys. J. C **5**, 461 (1998).
- [31] A. Bodek, and U. K. Yang, Modeling Neutrino and Electron Scattering Inelastic Cross Sections, hep-ex/0308007 (2003).
- [32] R. M. Barnett *et al.* (The Particle Data Group), Phys. Rev. D **54**, 165 (1996).
- [33] E. Friedman, A. Gal and J. Mares, Antiproton-nucleus potentials from global fits to antiprotonic X-rays and radiochemical data, Nucl. Phys. A **761**, 283 (2005).